
Diversifying Query: Region-Guided Transformer for Temporal Sentence Grounding

Xiaolong Sun^{1†}, Liushuai Shi^{1†}, Le Wang^{1*}, Sanping Zhou¹,
Kun Xia¹, Yabing Wang¹, Gang Hua²

¹National Key Laboratory of Human-Machine Hybrid Augmented Intelligence,
National Engineering Research Center for Visual Information and Applications,
Institute of Artificial Intelligence and Robotics, Xi'an Jiaotong University

²Wormpex AI Research

{sunxiaolong, shiliushuai, xiakun, wyb7wyb7}@stu.xjtu.edu.cn
{lewang, spzhou}@xjtu.edu.cn, ganghua@gmail.com

Abstract

Temporal sentence grounding is a challenging task that aims to localize the moment spans relevant to a language description. Although recent DETR-based models have achieved notable progress by leveraging multiple learnable moment queries, they suffer from overlapped and redundant proposals, leading to inaccurate predictions. We attribute this limitation to the lack of task-related guidance for the learnable queries to serve a specific mode. Furthermore, the complex solution space generated by variable and open-vocabulary language descriptions exacerbates the optimization difficulty, making it harder for learnable queries to distinguish each other adaptively. To tackle this limitation, we present a Region-Guided TRansformer (RGTR) for temporal sentence grounding, which diversifies moment queries to eliminate overlapped and redundant predictions. Instead of using learnable queries, RGTR adopts a set of anchor pairs as moment queries to introduce explicit regional guidance. Each anchor pair takes charge of moment prediction for a specific temporal region, which reduces the optimization difficulty and ensures the diversity of the final predictions. In addition, we design an IoU-aware scoring head to improve proposal quality. Extensive experiments demonstrate the effectiveness of RGTR, outperforming state-of-the-art methods on QVHighlights, Charades-STA and TACoS datasets.

1 Introduction

Temporal sentence grounding (TSG) aims at localizing the moment spans semantically aligned with the given language description in an untrimmed video. This area of research has drawn increasing attention in recent years due to its wide range of potential applications, such as human-computer interaction [30, 10] and information retrieval [22, 37]. Early methods address the TSG task by designing predefined dense proposals [6, 41, 35] or directly learning sentence-frame interactions [15, 16, 39]. The recent success of detection transformer (DETR) [2] has inspired the integration of transformers into the temporal sentence grounding framework [11, 24, 36]. By decoding moment spans from a set of learnable queries, they streamline the complicated grounding pipeline.

Although DETR-based approaches have achieved notable performance in TSG task, we still observe some unique limitations of the DETR structure compared to other fields (*i.e.*, object detection and

[†]Equal contribution.

^{*}Corresponding Author.

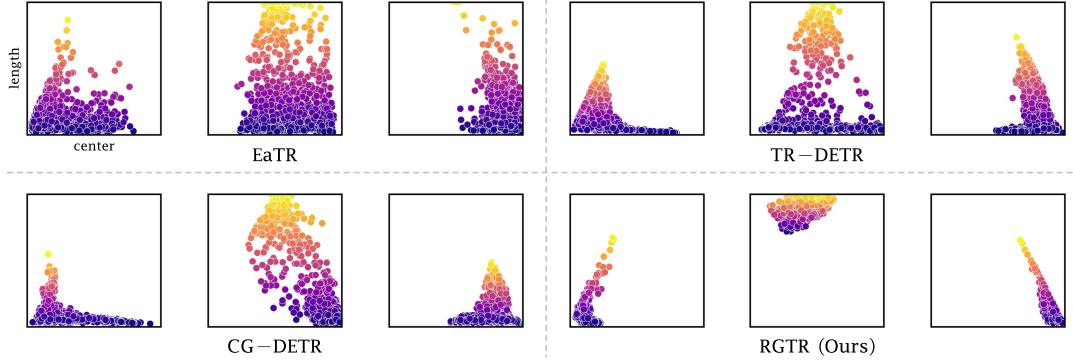


Figure 1: Visualization of all moment predictions on QVHighlights *val* split, for the 3 selected moment queries in EaTR [9], TR-DETR [31], CG-DETR [23] and RGTR (Ours). x-axis denotes the normalized moment span center coordinates, y-axis denotes the normalized moment span length. It can be observed that all queries in previous methods generate numerous overlapped and redundant proposals. For example, the second query tends to predict long moments near the middle of the videos, but the proposals of short moments conflict with this purpose, leading to inefficient predictions. In contrast, the predicted region of each query in our RGTR is distinct and more concentrated.

temporal action localization). Specifically, they suffer from limited query distribution and overlapped proposals, leading to inaccurate predictions. As shown in Fig. 1, we present the distribution of three representative moment queries in different methods, each query predicting different temporal regions (e.g., the lower left area represents a short moment near the video’s start and the higher middle area represents a long moment). In previous methods EaTR [9], TR-DETR [31] and CG-DETR [23], each query includes numerous overlapped and redundant proposals for the same region (i.e., the short moments in the lower part), resulting in inefficient predictions. We attribute this limitation to the lack of task-related guidance (e.g., category constraints, spatial distribution prior, etc.) for the learnable queries to serve a specific mode. The task-related guidance has been scarcely explored in TSG task although it is crucial to improve query diversity. Furthermore, the complex solution space generated by variable and open-vocabulary language descriptions exacerbates the optimization difficulty, making it harder for learnable queries to distinguish each other adaptively. Another limitation is that the proposal scoring in previous methods is purely based on the classification confidence (foreground or background), ignoring the quality of the predicted boundary. Instead, we argue that correctly classified proposals that better overlap with the ground-truth should be assigned higher scores. The above limitations significantly restrict the accurate localization of the DETR structure in TSG task.

In this paper, we introduce an effective Region-Guided TRansformer (RGTR) framework to cope with the aforementioned limitations in the TSG task. To address the issue of limited query diversity, we introduce regional priors based on the distribution of ground-truth moment spans as task-related guidance. Specifically, we design a region-guided decoder with a new concept of anchor pairs as moment queries to provide regional guidance. Each anchor pair consists of a static anchor and a dynamic anchor, both of which are initialized by different clustering points on the ground-truth moment spans. Such explicit initialization imposes the regional priors as guidance on each anchor pair, enhancing the diversity of the query distributions. The two types of anchors serve different roles in the decoder, collaboratively guiding localization with explicit regional guidance and eliminating overlapped predictions. In addition, to improve the scoring of high-quality proposals, we propose an IoU-aware scoring head. By supervising the IoU score with L2 loss, the prediction head considers both classification confidence and localization quality. As shown in Fig. 1, our RGTR eliminates redundant predictions and exhibits diverse query distributions compared to previous methods.

Our main contributions are summarized as follows. (1) We design a novel region-guided decoder, which adopts a set of explicitly initialized anchor pairs as moment queries to introduce regional priors as task-related guidance. (2) We propose an IoU-aware scoring head that incorporates localization quality to enhance classification confidence estimation and distinguish high-quality proposals. (3) By employing these techniques, we introduce a Region-Guided TRansformer that diversifies the moment

queries and improves proposal quality. Extensive experiments conducted on three challenging benchmarks demonstrate the superiority of the proposed model over state-of-the-art methods.

2 Related Works

Temporal Sentence Grounding in Videos. Temporal sentence grounding aims at predicting the moment spans of the described activity given an untrimmed video and a language description, which is first proposed in [6, 1]. Early methods fall into two main categories: proposal-based methods and proposal-free methods. Proposal-based methods [8, 17, 42, 35] initially generate multiple candidate proposals and rank them based on their similarity with the description. Despite achieving promising performance, these methods are greatly limited by the high computational cost of proposal matching. Proposal-free methods [3, 21, 16, 39] are proposed to avoid the need for predefined candidate moments. Instead of relying on segment candidates, they directly predict the start and end boundaries of the target moments by leveraging cross-modal interactions between video and sentence.

The recent success of detection transformer (DETR) [2] has inspired the integration of transformers into the temporal sentence grounding framework [11, 31, 24]. DETR-based methods simplify the whole process into an end-to-end manner by removing handcrafted techniques. However, due to the lack of task-related guidance for the learnable queries to serve a specific mode, almost all the previous methods generate numerous overlapped and redundant predictions. In contrast, our RGTR improves the diversity of queries and eliminates redundant predictions by introducing explicit regional priors.

Detection Transformers. Recently, Transformer [32] has raised great attention in computer vision [4, 33, 2]. The adoption of transformers to object detection (DETR) [2] builds a fully end-to-end object detection system based on transformers, which largely simplifies the traditional detection pipeline. It also achieves notable performances compared with highly optimized CNN-based detectors.

The formulation of decoder queries has been widely studied in previous works [44, 18, 28]. Anchor DETR [34] initializes queries based on anchor points for specific detection modes. DAB-DETR [18] formulates decoder queries with content and action embeddings. DINO [40] adds position priors for the positional query and randomly initializes the content query. Motivated by their great success, we introduce a set of anchor pairs to introduce the explicit regional priors for accurate prediction.

3 Method

In this section, we briefly present an overview of our proposed framework in Sec. 3.1. Then we elaborate on the main components of RGTR, including cross-modal alignment encoder (in Sec. 3.2), region-guided decoder (in Sec. 3.3) and IoU-aware scoring head (in Sec. 3.4). Finally, the training objectives are introduced in Sec. 3.5.

3.1 Overview

Given an untrimmed video $\mathcal{V} = \{v_t\}_{t=1}^L$ with L frames and an associated natural language description $\mathcal{T} = \{t_n\}_{n=1}^N$ with N words, Temporal Sentence Grounding (TSG) aims to accurately predict the moment span $\hat{m} = (\hat{m}_c, \hat{m}_\sigma)$ that is most relevant to the given text description, where \hat{m}_c and \hat{m}_σ represent the center time and duration length of the moment span.

Recent DETR-based methods [11, 24, 38] replace hand-crafted components with learnable positional queries to predict target moments. These positional queries, representing a set of learnable referential search areas, are initialized as random learnable embeddings in the previous methods [24, 38, 36]. However, due to the lack of task-related guidance (*e.g.*, categories constraints, spatial distribution prior, etc.) and the extensive variability of language descriptions, the random initialization of positional queries greatly exacerbates the optimization difficulty.

To address this problem, we propose a Region-Guided TRansformer (RGTR), which adopts a set of explicitly initialized anchor pairs to replace randomly initialized learnable queries without explicit guidance. In our framework, we construct a region-guided decoder through anchor pairs to provide directive and diverse reference search areas. In addition, we introduce an IoU-aware scoring head to distinguish high-quality proposals. The overall architecture is shown in Fig. 2.

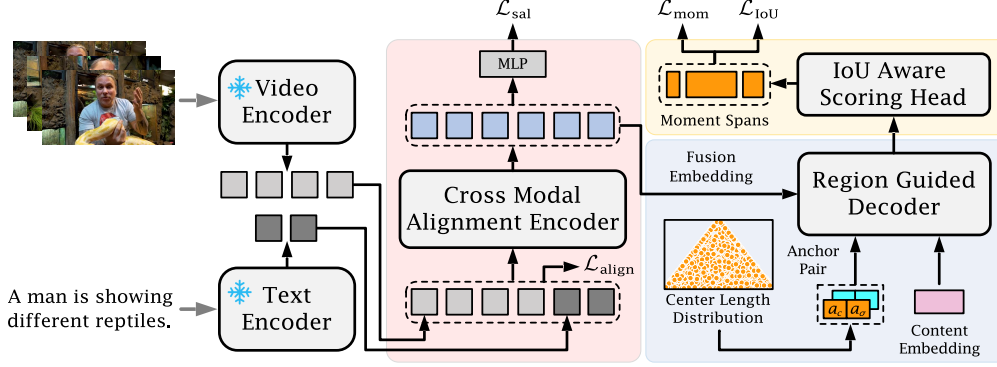


Figure 2: Overview of the proposed RGTR architecture. Given a video and a text description, we first employ two frozen pre-trained models to extract visual and textual features. Subsequently, the cross-modal alignment encoder is constructed to align and fuse the visual and textual features effectively. Then, we design a region-guided decoder to introduce the regional priors through a set of explicitly initialized anchor pairs. Finally, the IoU-aware scoring head generates high-quality moment spans by incorporating localization quality to enhance the classification confidence estimation.

3.2 Cross-Modal Alignment Encoder

Following previous methods [24, 31, 13], we use the pre-trained VGG model [29], CLIP [26] and Slowfast model [5] to extract clip-level visual features $F_v \in \mathbb{R}^{L \times d_v}$, where L represents the number of clips and d_v is the dimension of the visual features. Furthermore, we utilize the pre-trained Glove model [25] and CLIP model to extract word-level textual features $F_t \in \mathbb{R}^{N \times d_t}$, where N is the number of words and d_t is the dimension of the textual features.

Given the clip-level visual features F_v and the word-level textual features F_t , they are first projected into the common multimodal space using multi-layer perceptrons (MLPs) to produce the corresponding features $\bar{F}_v \in \mathbb{R}^{L \times D}$ and $\bar{F}_t \in \mathbb{R}^{N \times D}$, where D is the embedding dimension. As highlighted in previous work [12], aligning modalities before interaction could reduce the modal gap and obtain better modal representations. Therefore, we employ an alignment loss $\mathcal{L}_{\text{align}}$ to facilitate the alignment between videos and sentences by using their global representations.

$$\mathcal{L}_{\text{align}} = -\frac{1}{B} \sum_{i=1}^B \log \frac{\exp((G_v^i)(G_t^i)^\top)}{\sum_{i=1}^B \sum_{j=1}^B \exp((G_v^i)(G_t^j)^\top)}, \quad (1)$$

where B represents the batch size, $G_v^i \in \mathbb{R}^D$ and $G_t^i \in \mathbb{R}^D$ denote the global feature of the i -th video and the i -th sentence in a training batch, respectively. Additionally, we employ a visual feature refinement module [31] to suppress the interference of visual information irrelevant to the sentence.

After alignment, we adopt the text-to-video encoder [24] to obtain text-aware video representations. Specifically, three cross-attention layers are utilized to integrate textual features into the visual features, where query features are extracted from the visual features: $Q_v = \text{Linear}_q(\bar{F}_v)$, key and value features are obtained from the textual features $K_t = \text{Linear}_k(\bar{F}_t)$ and $V_t = \text{Linear}_v(\bar{F}_t)$:

$$\hat{F}_v = \text{Attention}(Q_v, K_t, V_t) = \text{Softmax}\left(\frac{Q_v K_t^\top}{\sqrt{D}}\right) V_t \in \mathbb{R}^{L \times D}. \quad (2)$$

Subsequently, three self-attention layers are leveraged to enhance the representations to help the model better understand the video sequence relations. Here, we project \hat{F}_v to $Q_{\hat{v}}$, $K_{\hat{v}}$ and $V_{\hat{v}}$ and use them to obtain the final cross-modal fusion embedding F , which is imposed by saliency score constraints \mathcal{L}_{sal} [31]. Refer to the supplemental material for detailed information about \mathcal{L}_{sal} .

3.3 Region-Guided Decoder

Given the cross-modal fusion embedding F , we aim to localize moment spans semantically aligned with the language description. As discussed in Sec. 3.1, previous methods employ randomly initialized learnable queries without explicit guidance, leading to increasing optimization difficulty and reduced query diversity. In contrast, we design a region-guided decoder, which adopts a set of explicitly initialized anchor pairs as moment queries to provide directive and diverse regional priors. Each anchor pair consists of a static anchor and a dynamic anchor, both of which are initialized by different clustering points on the ground-truth moment spans. The two anchors serve different roles in the decoder, collaboratively guiding localization with explicit regional guidance. The structure of the region-guided decoder is described in Fig. 3. We elaborate on the detailed process in the following.

Explicit anchor initialization. Due to the specificity of the TSG task, we lack the task-related guidance (*e.g.*, category constraints) present in other detection tasks. Nonetheless, we can still provide regional guidance for the decoding process by considering the distribution of ground-truth moment spans. Specifically, we first modify the 2D anchor boxes in [18] to represent 1D moments in the video, *i.e.*, the center coordinate m_c and the duration m_σ of the moments are utilized to represent the static anchor and dynamic anchor. Then, we generate \mathcal{K} representative points $A \in \mathbb{R}^{\mathcal{K} \times 2}$ by adopting k-means clustering algorithm on the ground-truth of all the moment spans $m = (m_c, m_\sigma)$ in the training dataset. These clustering points represent explicit temporal regions with diverse center coordinates and durations. Since events described in the sentence can occur anywhere in the video, generating diverse temporal regions as guidance is crucial. Therefore, the static and dynamic anchors are initialized to \mathcal{K} representative anchors: $A_s^0 = A_d^0 = A \in \mathbb{R}^{\mathcal{K} \times 2}$, and the positional embeddings of anchor pairs are generated by:

$$P_s^0 = P_d^0 = \text{MLP}(\text{PE}(A)), \quad (3)$$

where $\text{PE}(\cdot)$ means positional encoding to generate sinusoidal embeddings. For clarity, we use A_s^j and P_s^j to sign the static anchor in j -th decoder layer, even though they are never updated. With the explicit initialization, regional priors are introduced to guide different anchor pairs in generating non-overlapped predictions.

Anchor pair update. Although introducing regional guidance by explicit initialization, maintaining the guidance during decoding iterations is also important. Following this idea, the static anchor is designed to maintain guidance without updating, while the dynamic anchor is designed to update for localization. For static anchors, we have

$$A_s^{j+1} = A_s^0 = A, \quad P_s^{j+1} = P_s^0 = \text{MLP}(\text{PE}(A)). \quad (4)$$

Given the dynamic anchors $A_d^j = (a_c^j, a_\sigma^j)$ in j -th decoder layer and the relative positions $\Delta A_d^j = (\Delta a_c^j, \Delta a_\sigma^j)$ by a prediction head, the dynamic anchors and the positional embeddings are updated as:

$$A_d^{j+1} = A_d^j + \Delta A_d^j = (a_c^j + \Delta a_c^j, a_\sigma^j + \Delta a_\sigma^j), \quad P_d^{j+1} = \text{MLP}(\text{PE}(A_d^{j+1})). \quad (5)$$

Note that all prediction heads in different decoder layers share the same parameters.

Region-guided attention module. Similar to the general decoder, our region-guided decoder also includes two parts: self-attention module and cross-attention module. However, we employ different anchors in the two modules for varying roles, as shown in Fig. 3. In the self-attention module, we utilize static anchors to focus content embeddings on our preset representative temporal regions and share information across different regions, such that the updated content embedding C_s^j is as follows:

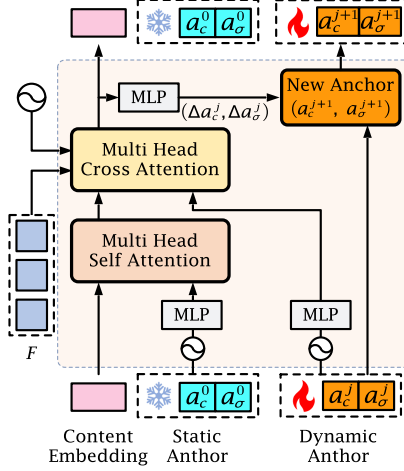


Figure 3: The structure of our proposed region-guided decoder with anchor pair (static anchor and dynamic anchor).

$$C_s^j = \text{Attention}(\text{Q} : C^{j-1} + P_s^0, \text{K} : C^{j-1} + P_s^0, \text{V} : C^{j-1}) \in \mathbb{R}^{\mathcal{K} \times D}, \quad (6)$$

where $C^{j-1} \in \mathbb{R}^{\mathcal{K} \times D}$ is the content embedding from $(j-1)$ -th decoder layer, and C^0 is initialized to zeros. In the cross-attention module, we employ dynamic anchors to aggregate region-specific features from cross-modal fusion embedding F with the assistance of region-guided content embedding C_s^j . Therefore, the content embedding C^j is updated as:

$$C^j = \text{Attention}(\text{Q} : \text{Cat}(C_s^j, P_d^j), \text{K} : \text{Cat}(F, \text{PE}(F)), \text{V} : F) \in \mathbb{R}^{\mathcal{K} \times D}, \quad (7)$$

where $\text{Cat}(\cdot)$ means concatenation function. By adopting anchor pairs with regional priors, the region-guided decoder ensures the diversity of the final predictions.

3.4 IoU-Aware Scoring Head

The region-guided decoder improves the quality of proposals by reducing overlapped and redundant proposals, while high-quality proposals demand not only fewer duplications but also accurate boundaries. In the previous DETR-based methods [24, 9, 31], classification confidence (foreground or background) is adopted to rank all final proposals. However, a single binary classification score may inadequately assess proposal quality by overlooking temporal boundary accuracy. To distinguish high-quality proposals, we introduce an IoU-aware scoring head, which considers both localization quality and classification confidence.

Specifically, the output of the decoder is fed to an FFN and a linear layer to predict the moment span $\hat{m} = (\hat{m}_c, \hat{m}_\sigma)$ and the confidence score p_c . Additionally, we add a linear layer to predict the expected IoU p_{IoU} with respect to the ground-truth IoU. Instead of scoring proposals by classification confidence alone, we score them by a joint combination of confidence and IoU score, *i.e.*, the product between p_c and p_{IoU} .

We supervise the IoU score with an L2 loss to the ground-truth IoU, denoted as \hat{g}_{IoU} ,

$$\mathcal{L}_{\text{IoU}} = ||p_{\text{IoU}} - \hat{g}_{\text{IoU}}||^2. \quad (8)$$

This additional IoU score can explicitly incorporate localization quality to enhance the classification confidence estimation, thereby generating high-quality proposals. In addition, non maximum suppression (NMS) is applied during the inference.

3.5 Training Objectives

The objective losses of RGTR include four parts: moment loss \mathcal{L}_{mom} , saliency loss \mathcal{L}_{sal} , alignment loss $\mathcal{L}_{\text{align}}$ and IoU loss \mathcal{L}_{IoU} . Following [24], moment loss includes L1, gIoU, and focal loss, and saliency loss includes margin ranking loss and contrastive loss. The overall objective is defined as:

$$\mathcal{L}_{\text{overall}} = \mathcal{L}_{\text{mom}} + \lambda_{\text{sal}}\mathcal{L}_{\text{sal}} + \lambda_{\text{align}}\mathcal{L}_{\text{align}} + \lambda_{\text{IoU}}\mathcal{L}_{\text{IoU}}, \quad (9)$$

where λ_* are the balancing parameters. Refer to the supplemental material for detailed information about the training objectives.

4 Experiments

4.1 Datasets, Metrics, and Implementation Details

Datasets. We evaluate the proposed method on three temporal grounding benchmarks, including the QVHighlights [11], Charades-STA [6], and TACoS [27] datasets. QVHighlights spans various themes from everyday lifestyle vlogs to social events in news videos. Charades-STA comprises intricate daily human activities. TACoS mainly showcases long-form videos focusing on culinary activities.

Metrics. To make fair comparisons, we adopt the Recall@1 (R1) under the IoU thresholds of 0.3, 0.5, and 0.7 following the previous works [11, 31, 23]. Since QVHighlights contains multiple

Table 1: Performance Comparison on QVHighlights *test* and *val* splits. We highlight the best score in each column in **bold**, and the second best score with underline.

Method	test					val				
	R1		mAP			R1		mAP		
	@0.5	@0.7	@0.5	@0.75	Avg.	@0.5	@0.7	@0.5	@0.75	Avg.
M-DETR [11] _{NeurIPS'21}	52.89	33.02	54.82	29.40	30.73	53.94	34.84	-	-	32.20
UMT [19] _{CVPR'22}	56.23	41.18	53.83	37.01	36.12	60.26	44.26	-	-	38.59
QD-DETR [24] _{CVPR'23}	62.40	44.98	62.52	39.88	39.86	62.68	46.66	62.23	41.82	41.22
UniVTG [14] _{ICCV'23}	58.86	40.86	57.60	35.59	35.47	59.74	-	-	-	36.13
EaTR [9] _{ICCV'23}	-	-	-	-	-	61.36	45.79	61.86	41.91	41.74
MomentDiff [13] _{NeurIPS'23}	57.42	39.66	54.02	35.73	35.95	-	-	-	-	-
TR-DETR [31] _{AAAI'24}	64.66	<u>48.96</u>	63.98	<u>43.73</u>	42.62	67.10	51.48	<u>66.27</u>	46.42	45.09
TaskWeave [38] _{CVPR'24}	-	-	-	-	-	64.26	50.06	65.39	<u>46.47</u>	45.38
UVCOM [36] _{CVPR'24}	63.55	47.47	63.37	42.67	<u>43.18</u>	65.10	51.81	-	-	<u>45.79</u>
CG-DETR [23] _{Arxiv'24}	<u>65.43</u>	48.38	<u>64.51</u>	42.77	42.86	<u>67.35</u>	<u>52.06</u>	65.57	45.73	44.93
RGTR (Ours)	65.50	49.22	67.12	45.77	45.53	67.68	52.90	67.38	48.00	46.95

Table 2: Performances on TACoS and Charades-STA. Video features are extracted using Slowfast and CLIP.

Method	TACoS				Charades-STA			
	R0.3	R0.5	R0.7	mIoU	R0.3	R0.5	R0.7	mIoU
2D-TAN [41]	40.01	27.99	12.92	27.22	58.76	46.02	27.50	41.25
M-DETR [11]	37.97	24.67	11.97	25.49	65.83	52.07	30.59	45.54
MomentDiff [13]	44.78	33.68	-	-	-	55.57	32.42	-
QD-DETR [24]	-	-	-	-	-	57.31	32.55	-
UniVTG [14]	51.44	34.97	17.35	33.60	<u>70.81</u>	<u>58.01</u>	<u>35.65</u>	50.10
CG-DETR [23]	<u>52.23</u>	<u>39.61</u>	<u>22.23</u>	<u>36.48</u>	70.43	58.44	36.34	<u>50.13</u>
RGTR (Ours)	53.04	40.31	24.32	37.44	72.04	57.93	35.16	50.32

Table 3: Results on Charades-STA with VGG backbone.

Method	R0.5	R0.7
2D-TAN [41]	40.94	22.85
FVMR [7]	42.36	24.14
SSRN [43]	46.72	27.98
UMT [19]	48.31	29.25
MomentDiff [13]	51.94	28.25
QD-DETR [24]	52.77	31.13
TR-DETR [31]	53.47	30.81
CG-DETR [23]	<u>55.22</u>	<u>34.19</u>
RGTR (Ours)	55.48	34.33

ground-truth moments per sentence, we also report the mean average precision (mAP) with IoU thresholds of 0.5, 0.75, and the average mAP over a set of IoU thresholds [0.5: 0.05: 0.95]. For Charades-STA and TACoS, we compute the mean IoU of top-1 predictions.

Implementation Details. Following previous methods [24, 13, 23], for all three datasets, we use SlowFast [5] and CLIP [26] to extract visual features and the text encoder in CLIP to extract textual features. In Charades-STA, we also extract visual features with VGG [29] and use Glove [25] for textual features. The cross-modal alignment encoder and region-guided decoder consist of three layers of transformer blocks. In the encoder, we also use a local regular loss following [31]. We set the embedding dimension D to 256 and the number of attention heads to 8. The number of anchor pairs \mathcal{K} is set to 20 for QVHighlights, 10 for Charades-STA and TACoS. The NMS threshold is set to 0.8. The balancing parameters are set as: $\lambda_{\text{align}} = 0.3$, $\lambda_{\text{iou}} = 1$, and λ_{sal} is set as 1 for QVHighlights, 4 for Charades-STA and TACoS. We train all the models with batch size 32 for 200 epochs using the AdamW optimizer [20] with weight decay $1e-4$ for all three datasets. The learning rate is set to $1e-4$.

4.2 Performance Comparison

As shown in Tab. 1, we compare RGTR to previous methods on QVHighlights. For a fair comparison, we report numbers for both the test and validation splits. Our RGTR achieves new state-of-the-art performance on all metrics. Specifically, RGTR outperforms the latest methods like CG-DETR, achieving 67.12% at mAP@0.5 and 45.77% at mAP@0.75 on the test dataset. Particularly, the average mAP score of 45.53% on the test dataset marks a significant improvement over UVCOM by 2.35%. On the validation dataset, RGTR also maintains its lead. The notable performance advantages of RGTR demonstrate the effectiveness of anchor pairs with explicit regional priors.

Tab. 2 and Tab 3 present comparisons on TACoS and Charades-STA. Our RGTR achieves the best performance on TACoS. On Charades-STA, RGTR also maintains its competitiveness regardless

Table 4: Ablation study on the components of RGTR on QVHighlights *val* split.

Explicit Anchor Initialization	Region-Guided Attention Module	IoU-Aware Scoring Head	R1		mAP		
			@0.5	@0.7	@0.5	@0.75	Avg.
			65.35	48.97	64.58	43.05	43.12
✓			64.65	50.58	64.98	45.50	44.82
		✓	66.19	49.61	65.06	44.43	44.03
✓	✓		65.55	51.29	65.96	46.08	45.36
✓		✓	66.13	51.68	66.31	47.55	46.51
✓	✓	✓	67.68	52.90	67.38	48.00	46.95

Table 5: Ablation study on distribution of anchor initialization.

Distribution	R0.5	R0.7	mAP _{avg}
random	66.19	49.61	44.03
uniform grids	67.10	50.97	44.93
k-means	67.68	52.90	46.95

Table 6: Ablation study on the IoU loss type.

Loss type	R0.5	R0.7	mAP _{avg}
Huber Loss	68.00	51.94	46.68
L1 Loss	66.65	51.89	46.73
L2 Loss	67.68	52.90	46.95

Table 7: Ablation study on various scoring methods.

Scoring	R0.5	R0.7	mAP _{avg}
IoU superv.	67.87	52.84	46.54
cls + IoU	67.23	52.39	46.92
cls × IoU	67.68	52.90	46.95

of whether 2D features (VGG) or multimodal pre-trained features (SF+C) are used. However, we observe that while our results are notably superior on QVHighlights, the margin is slightly reduced on TACoS and Charades-STA. We attribute this to the biased distribution on Charades-STA and TACoS compared to QVHighlights, resulting in less diversity learned by anchor pairs. We also provide results of RGTR on the anti-biased Charades-STA in the supplemental material.

4.3 Ablation Study

To investigate the impact corresponding to key components of the proposed method, we conduct ablation studies on the validation set of QVHighlights.

Component ablation. We first investigate the effectiveness of each component in our RGTR. As shown in Tab. 4, we report the impact according to explicit anchor initialization, region-guided attention module, and IoU-aware scoring head. The results demonstrate that each component contributes significantly to overall performance and using all components improves performance by 3.93% in terms of R1@0.7 and 3.83% in terms of mAP_{avg}.

Distribution of anchor initialization. We adopt another simple uniform sampling strategy to replace the k-means algorithm. Specifically, we first generate a uniform grid on the normalized $m_c \times m_\sigma$ area, and uniformly sample $5 \times 5 = 25$ anchor pairs in a practical temporal region. As shown in Tab. 5, the performance drops significantly when replacing the k-means algorithm with the uniform sampling for explicit anchor initialization. It verifies that our k-means algorithm can provide optimal explicit regional priors for the decoding process.

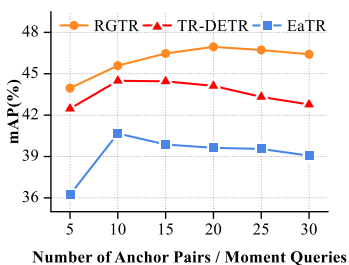


Figure 4: Ablation study on the number of moment queries \mathcal{K} .

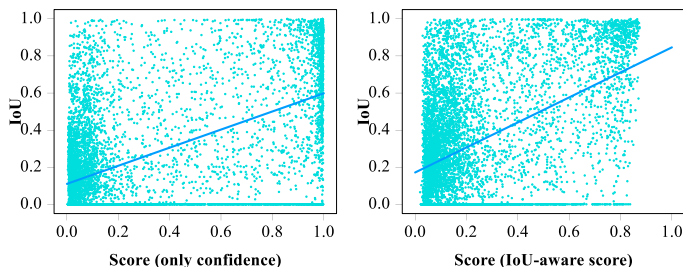


Figure 5: Correlation between scores and ground-truth IoUs on QVHighlights *val* split.

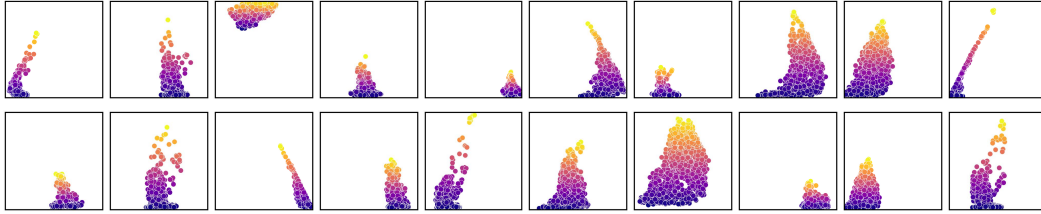


Figure 6: Visualization of all moment span predictions for all the videos on QVHighlights *val* split, for all the 20 moment queries in the region-guided decoder.

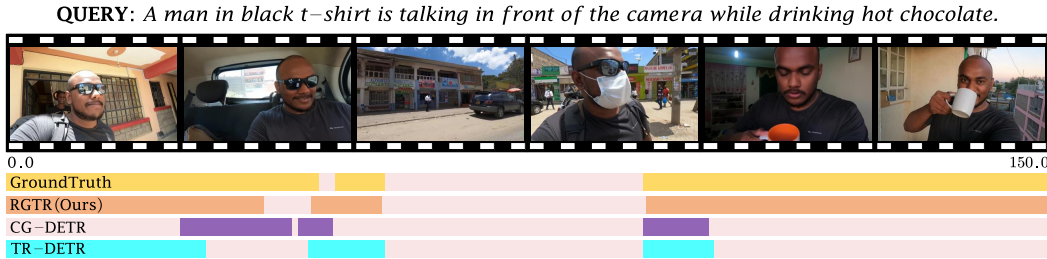


Figure 7: Visualization of prediction comparisons on QVHighlights.

IoU loss type. As shown in Tab. 6, we employ different IoU loss to supervise the IoU score. All loss types can significantly improve performance, among which L2 loss achieves optimal performance.

Various scoring methods. We utilize the product between classification confidence and IoU score as the final ranking criterion. Tab. 7 compares the product fusion with other methods, where IoU superv. means only using confidence score with IoU loss as supervision. All strategies have significant performance improvements, among which the product strategy achieves the best performance.

Number of anchor pairs. In the previous methods [24, 9, 31], the number of learnable positional queries \mathcal{K} is typically limited to 10. This is because increasing the number of positional queries without explicit guidance only produces more overlapped and redundant proposals, resulting in negligible performance improvement or even degradation. In contrast, our method provides explicit regional prior for each anchor pair, *i.e.*, each anchor pair is accountable for a specific temporal region. Therefore, increasing \mathcal{K} allows anchor pairs to cover more temporal regions, leading to effective prediction, rather than restricting \mathcal{K} to 10. As shown in Fig. 4, we present the performance of EaTR [9], TR-DETR [31], and our RGTR in terms of mAP_{avg} according to \mathcal{K} . We re-implement the other two methods by official codebase but in different \mathcal{K} . As discussed above, for TR-DETR and EaTR, performance peaks when \mathcal{K} reaches 10 and then declines significantly. In contrast, for RGTR, increasing \mathcal{K} to 20 significantly improves performance compared to 10, demonstrating the effectiveness of explicit regional guidance.

Correlation between scores and IoUs. To compare IoU-aware scoring and classification confidence scoring, we draw scatter plots of the correlation between scores and ground-truth IoUs on the QVHighlights validation set in Fig. 5. It can be observed that our IoU-aware score shows a stronger correlation with the ground-truth IoU, *i.e.*, the slope of the fitted line increases from 0.49 to 0.67, improving the distinction of high-quality proposals.

4.4 Visualization and Qualitative Result

As shown in Fig. 6, we visualize moment span predictions for all the 1550 QVHighlights *val* videos, for all the 20 moment queries in the region-guided decoder. Compared with previous methods in Fig. 1, RGTR introduces explicit regional guidance through anchor pairs, effectively eliminating numerous overlapped predictions and enhancing diversity.

In Fig. 7, we illustrate a qualitative example on QVHighlights, where the sentence corresponds to multiple moment spans. Since our method emphasizes enhancing prediction diversity, RGTR

generates more accurate moment predictions than other methods, especially in the case of requiring simultaneous attention to different center coordinates and durations.

5 Conclusion

In this paper, we propose a Region-Guided TRansformer (RGTR) framework to address the limitations of DETR structure in the TSG task. To improve the diversity of queries, we design a region-guided decoder, which adopts a set of anchor pairs as moment queries to introduce explicit regional guidance for the decoding process. Each anchor pair takes charge of moment prediction for a specific temporal region, which reduces the optimization difficulty and ensures the diversity of the final predictions. To distinguish high-quality proposals, we employ an IoU-aware scoring head that incorporates localization quality to enhance classification confidence estimation. Extensive experiments on three channeling benchmarks demonstrate the superiority of our proposed RGTR.

References

- [1] Anne Hendricks, L., Wang, O., Shechtman, E., Sivic, J., Darrell, T., Russell, B.: Localizing moments in video with natural language. In: Proceedings of the IEEE international conference on computer vision. pp. 5803–5812 (2017)
- [2] Carion, N., Massa, F., Synnaeve, G., Usunier, N., Kirillov, A., Zagoruyko, S.: End-to-end object detection with transformers. In: European conference on computer vision. pp. 213–229. Springer (2020)
- [3] Chen, L., Lu, C., Tang, S., Xiao, J., Zhang, D., Tan, C., Li, X.: Rethinking the bottom-up framework for query-based video localization. In: Proceedings of the AAAI Conference on Artificial Intelligence. vol. 34, pp. 10551–10558 (2020)
- [4] Dosovitskiy, A., Beyer, L., Kolesnikov, A., Weissenborn, D., Zhai, X., Unterthiner, T., Dehghani, M., Minderer, M., Heigold, G., Gelly, S., et al.: An image is worth 16x16 words: Transformers for image recognition at scale. arXiv preprint arXiv:2010.11929 (2020)
- [5] Feichtenhofer, C., Fan, H., Malik, J., He, K.: Slowfast networks for video recognition. In: Proceedings of the IEEE/CVF international conference on computer vision. pp. 6202–6211 (2019)
- [6] Gao, J., Sun, C., Yang, Z., Nevatia, R.: Tall: Temporal activity localization via language query. In: Proceedings of the IEEE international conference on computer vision. pp. 5267–5275 (2017)
- [7] Gao, J., Xu, C.: Fast video moment retrieval. In: Proceedings of the IEEE/CVF International Conference on Computer Vision. pp. 1523–1532 (2021)
- [8] Ge, R., Gao, J., Chen, K., Nevatia, R.: Mac: Mining activity concepts for language-based temporal localization. In: 2019 IEEE winter conference on applications of computer vision (WACV). pp. 245–253. IEEE (2019)
- [9] Jang, J., Park, J., Kim, J., Kwon, H., Sohn, K.: Knowing where to focus: Event-aware transformer for video grounding. In: Proceedings of the IEEE/CVF International Conference on Computer Vision. pp. 13846–13856 (2023)
- [10] Lan, L., Wang, X., Zhang, S., Tao, D., Gao, W., Huang, T.S.: Interacting tracklets for multi-object tracking. IEEE Transactions on Image Processing **27**(9), 4585–4597 (2018)
- [11] Lei, J., Berg, T.L., Bansal, M.: Detecting moments and highlights in videos via natural language queries. Advances in Neural Information Processing Systems **34**, 11846–11858 (2021)
- [12] Li, J., Selvaraju, R., Gotmare, A., Joty, S., Xiong, C., Hoi, S.C.H.: Align before fuse: Vision and language representation learning with momentum distillation. Advances in neural information processing systems **34**, 9694–9705 (2021)
- [13] Li, P., Xie, C.W., Xie, H., Zhao, L., Zhang, L., Zheng, Y., Zhao, D., Zhang, Y.: Momentdiff: Generative video moment retrieval from random to real. Advances in neural information processing systems **36** (2024)

- [14] Lin, K.Q., Zhang, P., Chen, J., Pramanick, S., Gao, D., Wang, A.J., Yan, R., Shou, M.Z.: Univtg: Towards unified video-language temporal grounding. In: Proceedings of the IEEE/CVF International Conference on Computer Vision. pp. 2794–2804 (2023)
- [15] Liu, D., Qu, X., Di, X., Cheng, Y., Xu, Z., Zhou, P.: Memory-guided semantic learning network for temporal sentence grounding. In: Proceedings of the AAAI Conference on Artificial Intelligence. vol. 36, pp. 1665–1673 (2022)
- [16] Liu, D., Qu, X., Hu, W.: Reducing the vision and language bias for temporal sentence grounding. In: Proceedings of the ACM International Conference on Multimedia. pp. 4092–4101 (2022)
- [17] Liu, M., Wang, X., Nie, L., Tian, Q., Chen, B., Chua, T.S.: Cross-modal moment localization in videos. In: Proceedings of the 26th ACM international conference on Multimedia. pp. 843–851 (2018)
- [18] Liu, S., Li, F., Zhang, H., Yang, X., Qi, X., Su, H., Zhu, J., Zhang, L.: Dab-detr: Dynamic anchor boxes are better queries for detr. arXiv preprint arXiv:2201.12329 (2022)
- [19] Liu, Y., Li, S., Wu, Y., Chen, C.W., Shan, Y., Qie, X.: Umt: Unified multi-modal transformers for joint video moment retrieval and highlight detection. In: Proceedings of the IEEE/CVF Conference on Computer Vision and Pattern Recognition. pp. 3042–3051 (2022)
- [20] Loshchilov, I., Hutter, F.: Decoupled weight decay regularization. arXiv preprint arXiv:1711.05101 (2017)
- [21] Lu, C., Chen, L., Tan, C., Li, X., Xiao, J.: Debug: A dense bottom-up grounding approach for natural language video localization. In: Proceedings of the 2019 Conference on Empirical Methods in Natural Language Processing and the 9th International Joint Conference on Natural Language Processing (EMNLP-IJCNLP). pp. 5144–5153 (2019)
- [22] Mao, Y., He, P., Liu, X., Shen, Y., Gao, J., Han, J., Chen, W.: Generation-augmented retrieval for open-domain question answering. In: Proceedings of the Annual Meeting of the Association for Computational Linguistics. pp. 4089–4100 (2021)
- [23] Moon, W., Hyun, S., Lee, S., Heo, J.P.: Correlation-guided query-dependency calibration in video representation learning for temporal grounding. arXiv preprint arXiv:2311.08835 (2023)
- [24] Moon, W., Hyun, S., Park, S., Park, D., Heo, J.P.: Query-dependent video representation for moment retrieval and highlight detection. In: Proceedings of the IEEE/CVF Conference on Computer Vision and Pattern Recognition. pp. 23023–23033 (2023)
- [25] Pennington, J., Socher, R., Manning, C.D.: Glove: Global vectors for word representation. In: Proceedings of the 2014 conference on empirical methods in natural language processing (EMNLP). pp. 1532–1543 (2014)
- [26] Radford, A., Kim, J.W., Hallacy, C., Ramesh, A., Goh, G., Agarwal, S., Sastry, G., Askell, A., Mishkin, P., Clark, J., et al.: Learning transferable visual models from natural language supervision. In: International conference on machine learning. pp. 8748–8763. PMLR (2021)
- [27] Regneri, M., Rohrbach, M., Wetzell, D., Thater, S., Schiele, B., Pinkal, M.: Grounding action descriptions in videos. *Transactions of the Association for Computational Linguistics* **1**, 25–36 (2013)
- [28] Shi, S., Jiang, L., Dai, D., Schiele, B.: Motion transformer with global intention localization and local movement refinement. *Advances in Neural Information Processing Systems* **35**, 6531–6543 (2022)
- [29] Simonyan, K., Zisserman, A.: Very deep convolutional networks for large-scale image recognition. arXiv preprint arXiv:1409.1556 (2014)
- [30] Singha, J., Roy, A., Laskar, R.H.: Dynamic hand gesture recognition using vision-based approach for human–computer interaction. *Neural Computing and Applications* **29**(4), 1129–1141 (2018)

- [31] Sun, H., Zhou, M., Chen, W., Xie, W.: Tr-detr: Task-reciprocal transformer for joint moment retrieval and highlight detection. arXiv preprint arXiv:2401.02309 (2024)
- [32] Vaswani, A., Shazeer, N., Parmar, N., Uszkoreit, J., Jones, L., Gomez, A.N., Kaiser, Ł., Polosukhin, I.: Attention is all you need. *Advances in neural information processing systems* **30** (2017)
- [33] Wang, X., Girshick, R., Gupta, A., He, K.: Non-local neural networks. In: *Proceedings of the IEEE conference on computer vision and pattern recognition*. pp. 7794–7803 (2018)
- [34] Wang, Y., Zhang, X., Yang, T., Sun, J.: Anchor detr: Query design for transformer-based detector. In: *Proceedings of the AAAI conference on artificial intelligence*. vol. 36, pp. 2567–2575 (2022)
- [35] Wang, Z., Wang, L., Wu, T., Li, T., Wu, G.: Negative sample matters: A renaissance of metric learning for temporal grounding. In: *Proceedings of the AAAI Conference on Artificial Intelligence*. vol. 36, pp. 2613–2623 (2022)
- [36] Xiao, Y., Luo, Z., Liu, Y., Ma, Y., Bian, H., Ji, Y., Yang, Y., Li, X.: Bridging the gap: A unified video comprehension framework for moment retrieval and highlight detection. arXiv preprint arXiv:2311.16464 (2023)
- [37] Yadav, V., Bethard, S., Surdeanu, M.: Unsupervised alignment-based iterative evidence retrieval for multi-hop question answering. In: *Proceedings of the Annual Meeting of the Association for Computational Linguistics*. pp. 4514–4525 (2020)
- [38] Yang, J., Wei, P., Li, H., Ren, Z.: Task-driven exploration: Decoupling and inter-task feedback for joint moment retrieval and highlight detection. arXiv preprint arXiv:2404.09263 (2024)
- [39] Yang, S., Wu, X.: Entity-aware and motion-aware transformers for language-driven action localization. In: *Proceedings of the Thirty-First International Joint Conference on Artificial Intelligence*, LD Raedt, Ed. pp. 1552–1558 (2022)
- [40] Zhang, H., Li, F., Liu, S., Zhang, L., Su, H., Zhu, J., Ni, L.M., Shum, H.Y.: Dino: Detr with improved denoising anchor boxes for end-to-end object detection. arXiv preprint arXiv:2203.03605 (2022)
- [41] Zhang, S., Peng, H., Fu, J., Luo, J.: Learning 2d temporal adjacent networks for moment localization with natural language. In: *Proceedings of the AAAI Conference on Artificial Intelligence*. vol. 34, pp. 12870–12877 (2020)
- [42] Zhang, S., Su, J., Luo, J.: Exploiting temporal relationships in video moment localization with natural language. In: *Proceedings of the 27th ACM International Conference on Multimedia*. pp. 1230–1238 (2019)
- [43] Zhu, J., Liu, D., Zhou, P., Di, X., Cheng, Y., Yang, S., Xu, W., Xu, Z., Wan, Y., Sun, L., et al.: Rethinking the video sampling and reasoning strategies for temporal sentence grounding. arXiv preprint arXiv:2301.00514 (2023)
- [44] Zhu, X., Su, W., Lu, L., Li, B., Wang, X., Dai, J.: Deformable detr: Deformable transformers for end-to-end object detection. arXiv preprint arXiv:2010.04159 (2020)